Capturing 3D Mode Shapes with Cell Phone Videos

Shawn Richardson, Mark Richardson
Vibrant Technology, Inc., Centennial, CO

Click here for the IMAC Power Point presentation

ABSTRACT

Everyone has a cell phone in their pocket which has a video camera in it. A cell phone video is a low-cost, non-contacting way of recording the vibration of rotating machinery and the resonant vibration of mechanical structures. A cell phone video is a quick way to visualize vibration and complement other **ODS** and **Modal** testing methods.

For this paper, **ODS-FRF** measurement functions were calculated from time waveforms (**TWFs**) that were extracted from cell phone videos of a rotating machine. Then the **ODS-FRFs** were curve fit using **FRF-based** curve fitting to yield **2D OMA** mode shapes of the machine. Two sets of **2D OMA** mode shapes were obtained from videos recorded at ***right angle views*** of the machine, two from the **Side** and two from the **Top**.

First, two different **shape correlation methods** were used to confirm the validity of the **2D** mode shapes obtained from the **two videos of each view**.

Then, **3D mode shapes** were created for each view by adding mode shape components for their missing third direction using components from the **2D mode shapes** from the other view. The only requirement for preserving the magnitudes & phases of the missing mode shape components is that the **ODS-FRFs** share a ***common reference*** **DOF**.

KEY WORDS

Time Waveform (**TWF**), Digital Fourier Transform (**DFT**), Auto Power Spectrum (**APS**), Cross Power Spectrum (**XPS**). **ODS-FRF, OMA** (Operational Modal Analysis) mode shape, **FEA** (Finite Element Analysis) mode shape, **Video ODS** animation

ROTATING MACHINE

The test article used for this paper is shown on Figure 1. The machine speed remained at ***approximately*** **1000 RPM** throughout all the cell phone video recordings.

All cell phone videos were recorded with one unbalancing screw added to each machine rotor. Previous papers [1], [2] presented results where different numbers of screws were added to the rotors of a similar rotating machine to create different unbalance cases and uniquely identify them using ODS's and mode shapes obtained from cell phone videos.

Figure 1. Rotating Machine With Unbalance Screws Added to Its Rotors

INTRODUCTION

The traditional method of measuring machine vibration using accelerometers and multichannel data acquisition is more expensive and time-consuming to implement compared to recording a cell phone video. Furthermore, because it is non-contacting, a cell phone video can record vibration of structural parts that are too hot, too dangerous, or are not accessible for attaching accelerometers.

In a previous paper [2], **3D** mode shapes were created by curve fitting **FEA** mode shapes to the **2D OMA** mode shapes of a rotating machine. That approach also showed how ***several* FEA *mode shapes participate*** in each order-based mode shape obtained from a cell phone video. In this paper, **3D OMA** mode shapes are created by combining mode shape components obtained from two cell phone videos recorded at right-angle-views of a rotating machine.

TWFs & DFTs

When a **raw video** is processed in MEscope [10], a **rectangular grid** of points is created and the horizontal & vertical deflections of ***millions of pixels*** in each frame of the **raw video** are processed to extract **TWFs** of the horizontal & vertical deflections of ***thousands of points*** in the point grid.

Time-based ODS's are displayed in animation by sweeping a **Line** cursor through the **TWFs**. A **DFT** is calculated from each **TWF**, and **frequency-based ODS's** are displayed in animation using **sinusoidal modulation** of the **ODS** at a cursor position in the **DFTs**. These **Video ODS** animations allow vibration to be ***visualized at slower speeds*** with ***higher deflection amplitudes***.

Using a point grid, the **magnitude & phase** of an **ODS** at selected grid points can be displayed during a **Video ODS** animation, as shown in Figures 2 & 3.

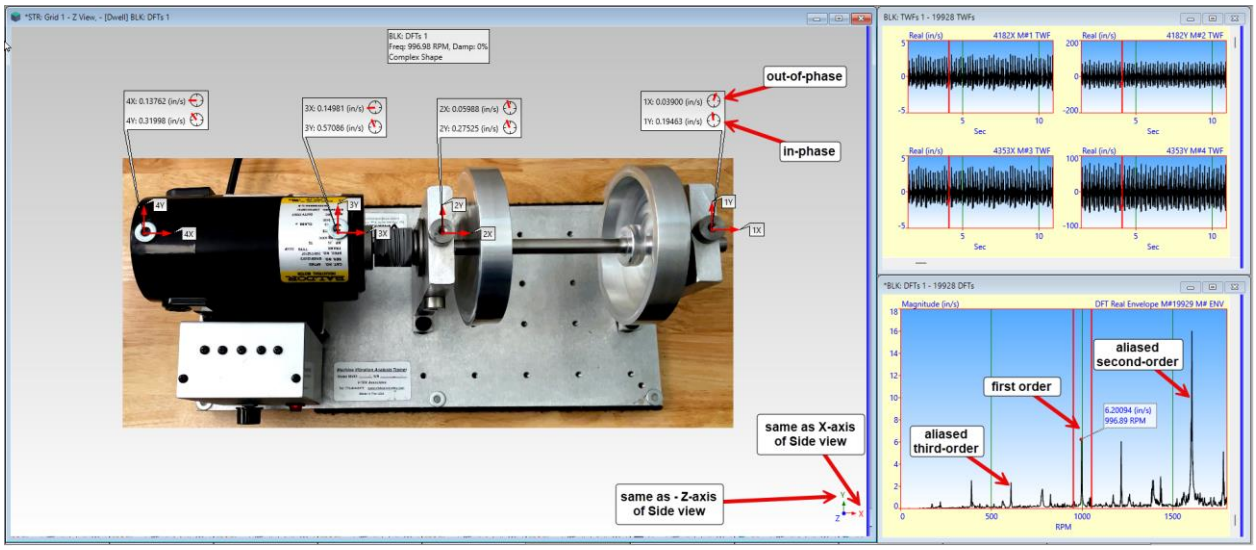

Figure 2. Top View of the First-Order ODS Animated from DFTs

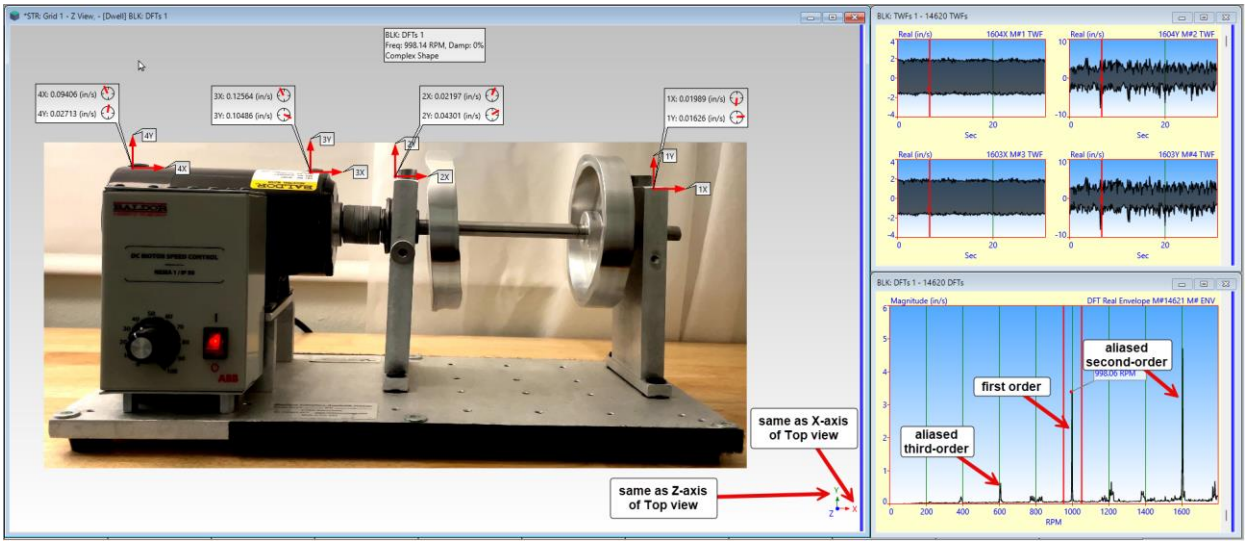

Figure 3. Side View of the First-Order ODS Animated from DFTs

The magnitudes & phases of the **ODS** extracted from the **Top** view video in Figure 2 show that the motor is vibrating at **0.57 in/s** in the **Y**-direction at the drive end of the motor. The magnitudes & phases also show that the bearing blocks are **in-phase** with the motor in the **Y**-direction and are **90 degrees out-of-phase** with the motor in the **X**-direction.

ALIASED ORDER PEAKS

No low-pass filtering is used to remove high-frequency vibration signals from a raw video recording.

Without low-pass filtering, machine resonance peaks at ***frequencies above one-half of the video recording frequency, (the fps camera setting)***, are ***folded around one-half of the fps***, (called **Fmax**), and appear at frequencies below **Fmax** in the **DFTs**. Aliased order peaks are shown in both Figures 2 & 3.

All machine-order resonance peaks between **Fmax & 2x Fmax** are folded around (***wrapped around***) **Fmax** and appear at lower frequencies in the frequency band **(0 to Fmax)**. Aliasing of higher frequencies occurs in ***all frequency domain functions***, including **DFTs** and **ODS-FRFs**.

The ***magnitude envelope*** of the **DFTs** is shown in Figures 2 & 3. Each **DFT** was calculated from a **TWF** that was extracted from a raw video that was sampled at **60 fps**, or **3600 RPM**. Therefore, **Fmax** of the **DFTs** is **1800 RPM**.

The first-order peak at the machine's running speed is clearly visible ***at approximately*** **1000 RPM**. The **second order peak** should be at about **2000 RPM,** and the **third order peak** at about **3000 RPM, etc.** The aliased frequency of an order higher than **Fmax** can be calculated from **Fmax** and its expected order frequency.

- **Second order** aliased frequency: (2000-1800) = 200 ➔ 1800-200 = **1600 RPM**
- **Third order** aliased frequency: (3000-1800) = 1200 ➔ 1800-1200 = **600 RPM**
- **Fourth order** aliased frequency: (4000-3600) = 400 ➔ 3600-400 = 3200 ➔ 3200-1800 = 1400 ➔ (1800-1400) = **400 RPM**

Aliased order peaks for the **second & third orders** are ***clearly visible at their aliased frequencies*** in the **DFTs**. The aliased **2000 RPM** order appears at **1600 RPM**, and the aliased **3000 RPM** order appears at **600 RPM**. Other peaks in the **DFTs** are evidence of aliased higher orders or structural resonances.

ODS-FRFs

A unique frequency domain function, called an **ODS-FRF,** can be calculated from each **TWF** extracted from a video. ***Spectrum averaging*** is used to remove random noise and non-linearities which appear as random noise from an **ODS-FRF**. **Hanning** windowing is also used to ***reduce signal leakage*** from the resonance peaks and to enable **FRF-based** curve fitting.

The ***magnitude*** of an **ODS-FRF** is the **APS** of a ***response*** **DOF** at a grid point. The ***phase*** of an **ODS-FRF** is the ***phase*** of the **XPS** between the ***response*** **DOF** and a ***reference*** **DOF** of the point grid.

An **ODS-FRF** has ***units of displacement***, which are the same as the **TWF** from which it is calculated.

An **ODS-FRF** can be ***differentiated to velocity units*** by multiplying it by the frequency variable. Vibration in ***velocity units*** is commonly used to quantify vibration levels in rotating equipment.

One of the laws of the **FFT** algorithm is $\Delta\mathbf{f} = \mathbf{1/T}$, where $\Delta\mathbf{f}$ is the ***frequency resolution between samples*** of an **ODS-FRF**, and **T** is the ***time length*** of **TWF** data from which the **ODS-FRF** was calculated. For example, if an **ODS-FRF** is calculated from a **TWF** using **25 second**s of uniformly sampled data, the frequency resolution ($\Delta\mathbf{f}$) of the **ODS-FRF** is **60/25** or **2.4 RPM**.

To increase the frequency resolution, (reduce $\Delta\mathbf{f}$), of an **ODS-FRF**, **TWF** data must be acquired over a ***longer period*** **T**. This means that the raw video from which **TWFs** are extracted must be recorded over a ***longer period*** **T**.

ODS-FRFs From the Motor and Bearing Blocks

ODS-FRFs were calculated from the **TWFs** for four selected points. two on the top of the motor, and one on the top of each bearing block, as shown in Figures 2 & 3. The **ODS-FRFs** were calculated using **1600 TWF** samples per average, 5 spectrum averages, and a Hanning window was applied to each average to reduce leakage from the resonance peaks.

The magnitude & phase of a typical **ODS-FRF** are shown in Figure 4.

Notice that the **first & aliased second order peaks** are at their expected frequencies, but there is a peak at about **500 RPM** which is not the aliased frequency of the third or fourth order. None the less, this resonance peak can be curve fit to obtain its **OMA** mode shape just like the order-based resonance peaks.

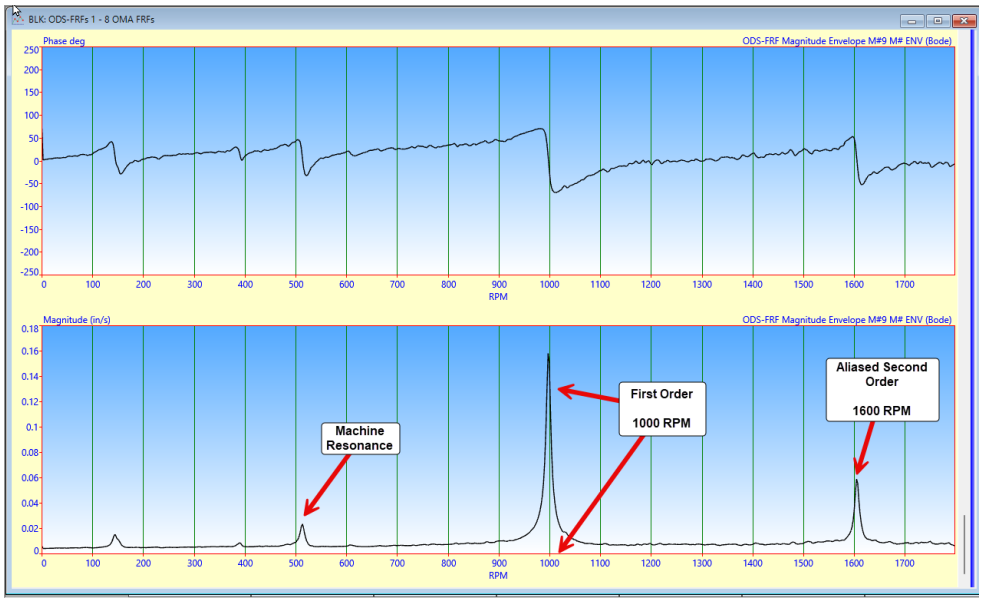

Figure 4. ODS-FRF Showing First Order & Aliased Second Order Peak

CURVE FITTING THE ODS-FRFS

If they have been windowed with a special window beforehand, **ODS-FRFs** can be curve-fit using an **FRF-based curve fitter**. This window is called a **Deconvolution window** in MEscope [10].

OMA mode shapes can be obtained from a set of **ODS-FRFs** if they are windowed using a **Deconvolution window** ***before*** **FRF-based curve fitting** is applied to them.

An **FRF-based curve fit** of an **ODS-FRF** is shown in Figure 5. In the left-hand graph, the **red curve fitting function** is overlaid on the magnitude & phase plots of the **ODS-FRF**.

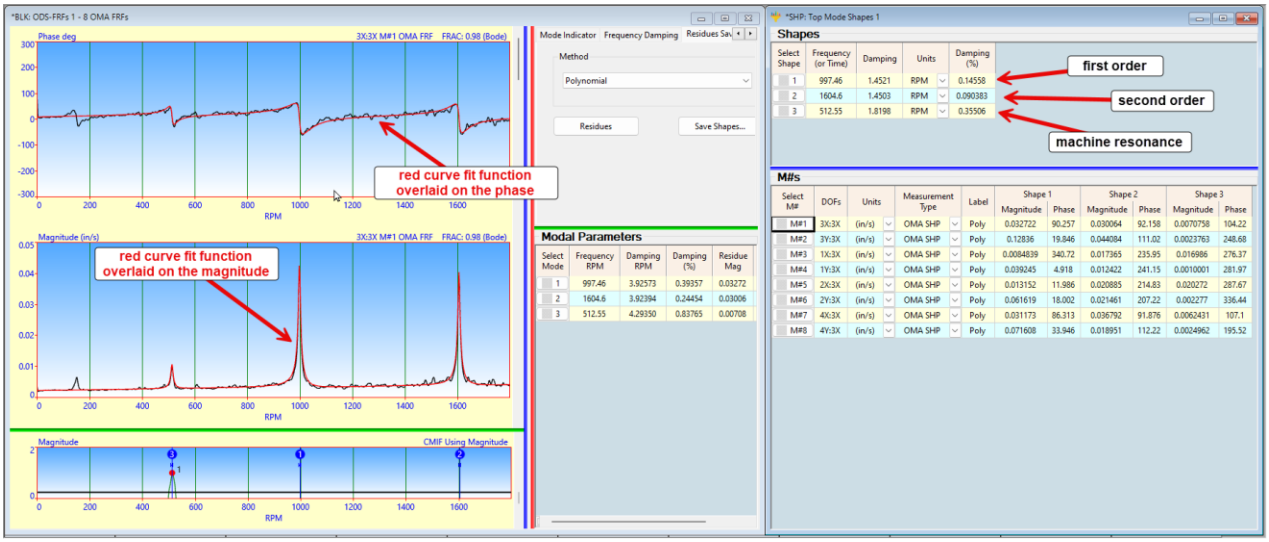

Figure 5. Curve Fit of an ODS-FRF

MAC & SDI CORRELATION COEFFICIENTS

OMA mode shapes were obtained from two video recordings of a **Side** view and from two video recordings of the **Top** view of the rotating machine. Each mode shape has eight complex-valued components which are the X & Y deflections at the four chosen grid points, two on the motor, and one on the top of each bearing block.

To confirm the validity of the mode shapes obtained from ***two videos of the same view***, the mode shapes were correlated with one another using two different shape correlation coefficients, the **Modal Assurance Criterion** (**MAC**) and the **Shape Difference Indicator** (**SDI**).

Both **MAC** & **SDI** have values **between 0 & 1**. A value of **"1"** means that ***two mode shapes are the same***. A **MAC** or **SDI** value ***less than*** **"0.9"** means that ***two shapes are different*** from one another.

The **MAC** & **SDI** values between the **OMA** mode shapes from the two **Side** view videos are shown in Figure 6 and from the two **Top** view videos in Figure 7.

MAC & SDI - 2D MODE SHAPES FROM TWO VIDEOS

In Figure 6, the mode shapes obtained from two **Side** view videos correlate well, with ***all diagonal*** **MAC** & **SDI** ***values above*** **90%.** The low ***off-diagonal*** **MAC** & **SDI** values indicate that each **OMA** mode shape has magnitudes & phases that are different from those of the other two mode shapes.

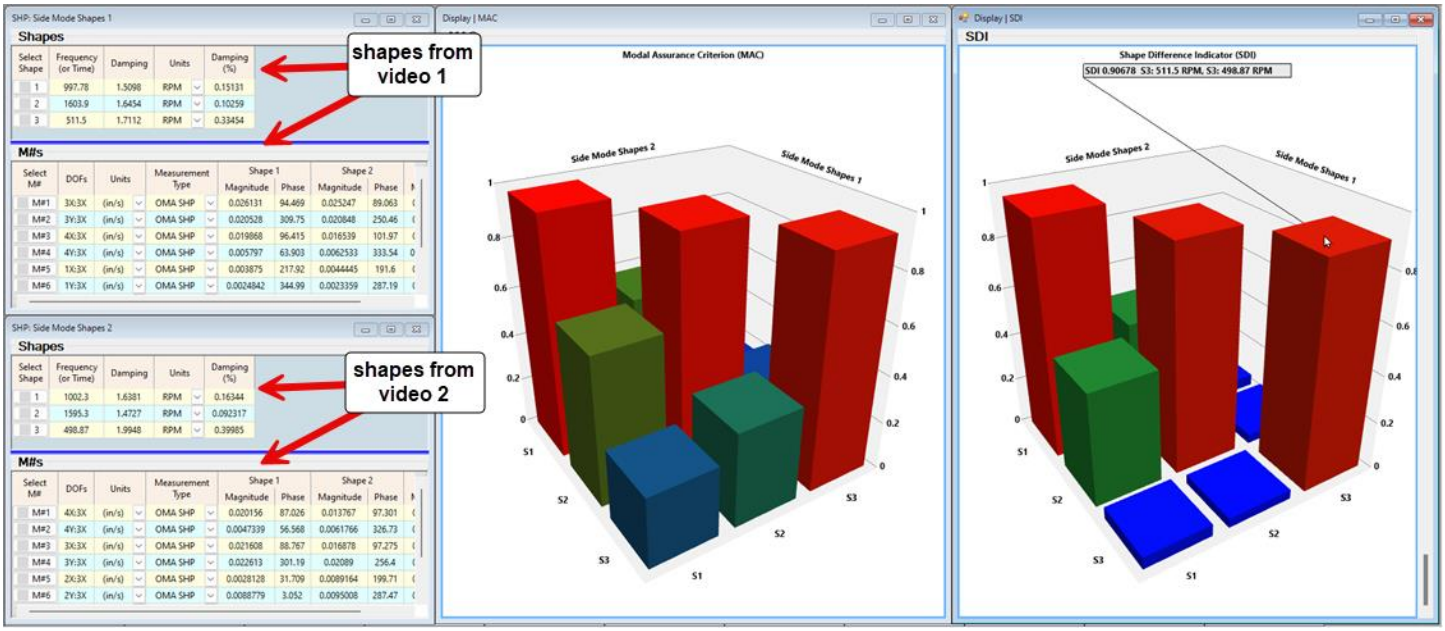

Figure 6. MAC & SDI of 2D Mode Shapes From Two Side View Videos

In Figure 7, the mode shapes from two **Top** view videos of the rotating machine are correlated using **MAC** & **SDI**. All three mode shapes obtained from the two **Top** view videos correlate with ***diagonal*** **MAC** & **SDI** ***values above*** **95%.**

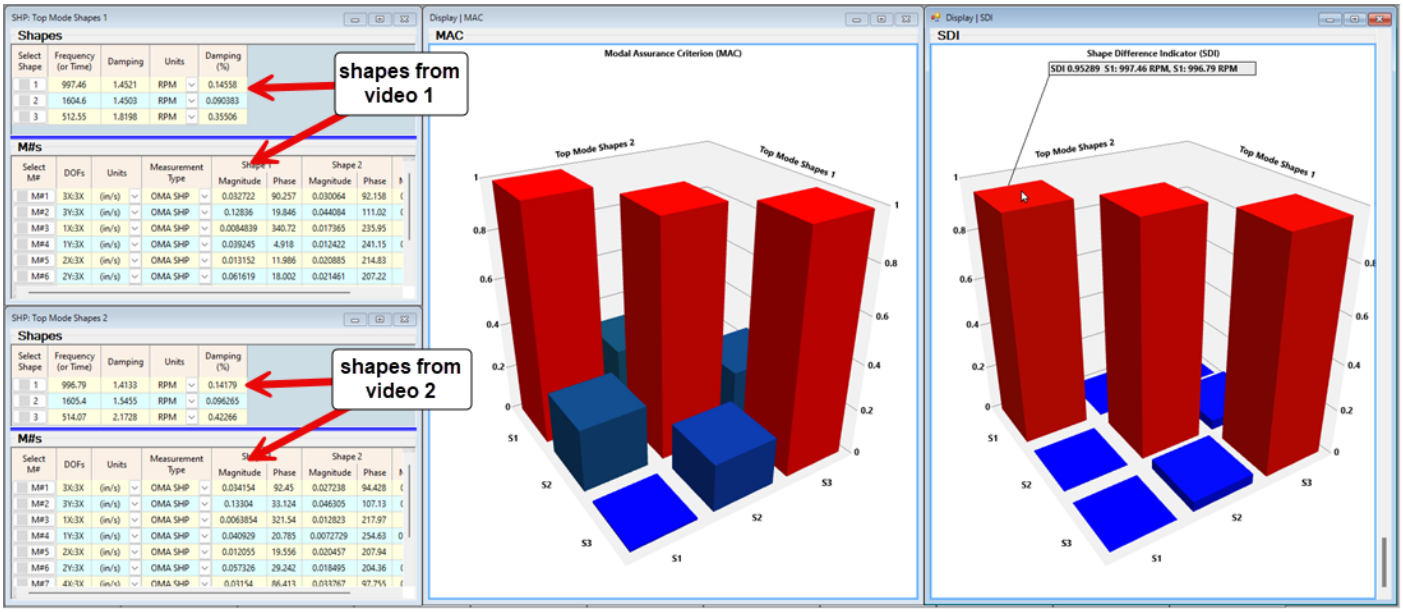

Figure 7. MAC & SDI - 2D Mode Shapes From Two Top View Videos

CREATING 3D MODE SHAPES USING A COMMON DOF

It can be seen from Figures 2 & 3 that the **X-axis**, (the direction of the shaft of the machine), is the same in both the **Side** & **Top** views. Therefore, residue mode shape components derived from **ODS-FRFs** ***with the same reference*** **DOF** can be copied from the mode shapes from one view to the mode shapes of the other view. In this case, **3X**, (the horizontal motion of point 3 on the motor), was used as the **reference DOF** for calculating **ODS-FRFs** from both the **Top** and **Side** views of the machine.

From inspection of Figure 2, the **Y-direction** of motion in the **Top** view is the same as the **negative Z-direction** in the **Side** view. From inspection of Figure 3, the **Y-direction** of motion in the **Side** is the same as the **Z-direction** of motion in the **Top** view.

Therefore, **3D** mode shapes for the **Side** view were created by adding the **Y-direction** mode shape components from the **2D** mode shapes from the **Top** view to the **2D** mode shapes from the **Side** view with ***negative*** **Z-direction roving DOFs**.

Likewise, **3D** mode shapes for the **Top** view were created by adding the **Y-direction** mode shape components from the **2D** mode shapes from the **Side** view to the **2D** mode shapes from the **Top** view with **Z-direction roving DOFs**.

The **2D** mode shapes from the **Top** view are shown on the left side in Figure 8. The **selected Y-direction DOFs** from the Side view are shown in the middle, and the **3D** mode shapes of the **Top** view are shown on the right side of Figure 8.

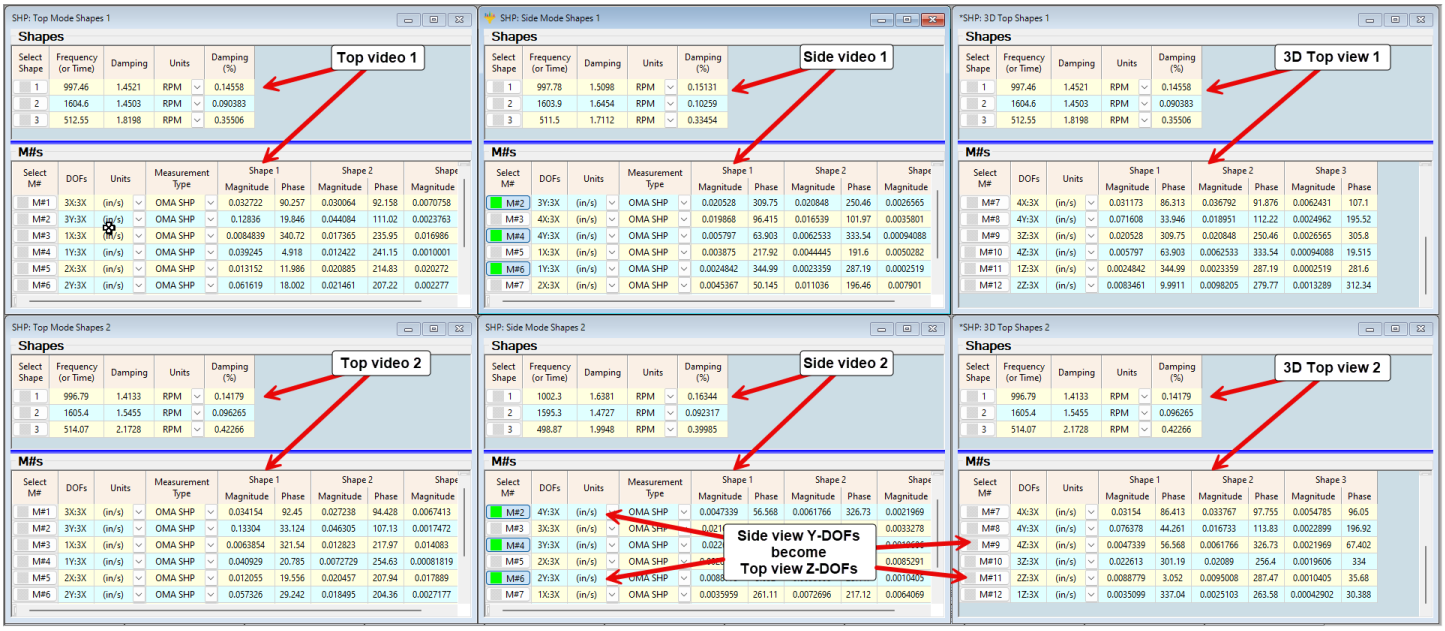

Figure 8 2D Top View Mode Shapes, Selected Side View DOFs, and 3D Top View Mode Shapes

ANIMATED DISPLAY - 3D MODE SHAPES FROM TWO SIDE VIEW VIDEOS

In Figure 9, the magnitudes & phases of the first-order **3D** mode shape from both **Side** view videos are shown during shape animation. In the **X**-direction, the **motor and inner bearing block** are ***in-phase with one another***, and the **motor and outer bearing block** are **180** ***degrees out-of-phase*** with one another. In the **Y**-direction, the **front end of the motor** is ***in-phase*** with both bearing blocks and the **back end of the motor** is ***90 degrees out-of-phase*** with both bearing blocks. In the **Z-direction**, **both ends of the motor and both bearing blocks** are ***all in-phase with one another***, indicating a ***rocking motion*** of the machine in the **Z**-direction.

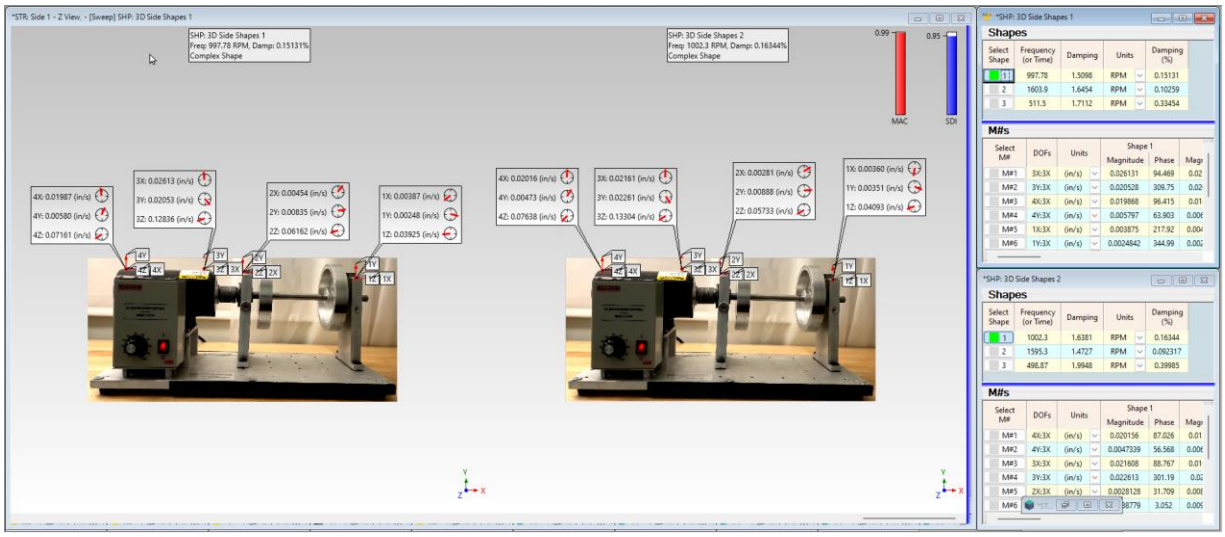

Figure 9 Animated Deflection of the First-Order 3D Mode Shapes From Both Side View Vidoes

ANIMATED DISPLAY - 3D MODE SHAPES FROM TWO TOP VIEW VIDEOS

In Figure 10, the magnitudes & phases of the first-order **3D** mode shape from both **Top** view videos are shown during shape animation. In the **X**-direction, the **motor** is ***90 degrees out-of-phase*** with **both bearing blocks**. In the **Y-direction**, the motor and both bearing blocks are ***in-phase*** with one another. This agrees with the ***rocking motion*** of deflection in the **Z-direction** of the **3D** mode shapes from the **Side** view. In the **Z-direction**, the **front end** of the motor is ***in-phase*** with **both bearing blocks** and the **back end** is ***out-of-phase***. This agrees with the **Y-direction** of deflection of the **3D** mode shapes from the **Side** view.

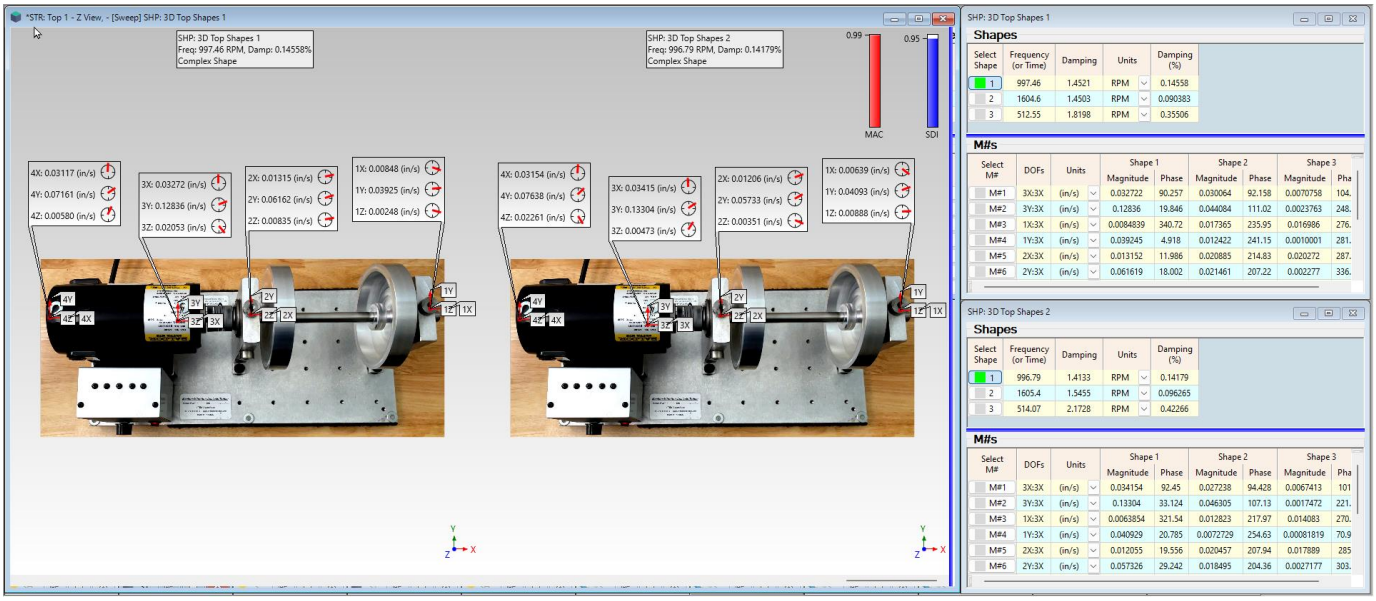

Figure 10. Top View - Animated Deflection of the First-Order 3D Mode Shapes

MAC & SDI - 3D MODE SHAPES FROM TWO TOP VIEW VIDEOS

In Figure 11, the **MAC & SDI** values of the **3D** mode shapes from the two **Top** view videos correlated with ***diagonal*** **MAC** & **SDI** values ***above*** **95%.** The ***low off-diagonal*** **MAC** & **SDI** values indicate that the **magnitudes & phases** of each mode shape are ***quite different*** compared with the other two mode shapes.

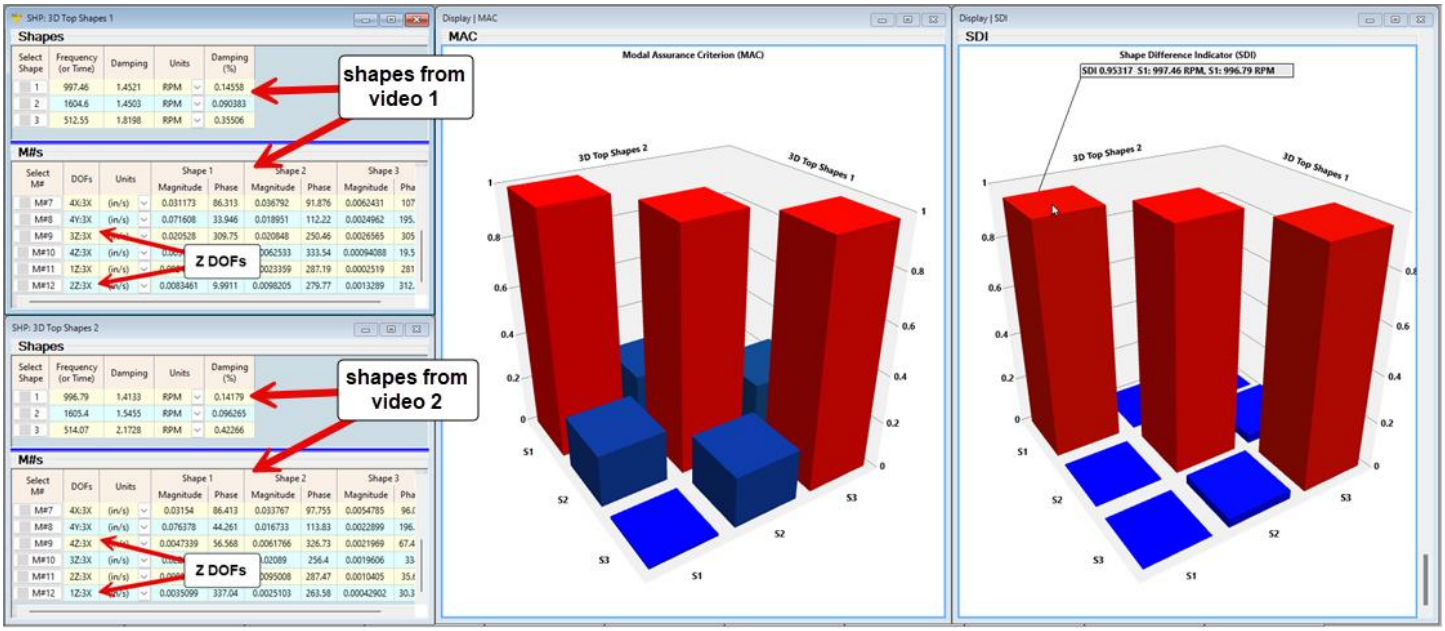

Figure 11. MAC & SDI - 3D Mode Shapes From Two Top View Videos

MAC & SDI - 3D MODE SHAPES FROM TWO SIDE VIEW VIDEOS

In Figure 12, the **MAC & SDI** values of the **3D** mode shapes from the two **Side** view videos correlated with ***diagonal*** **MAC** & **SDI** values ***above*** **90%**, except the **500 RPM** machine resonance mode shape which correlated with an **SDI** value of **87%.**

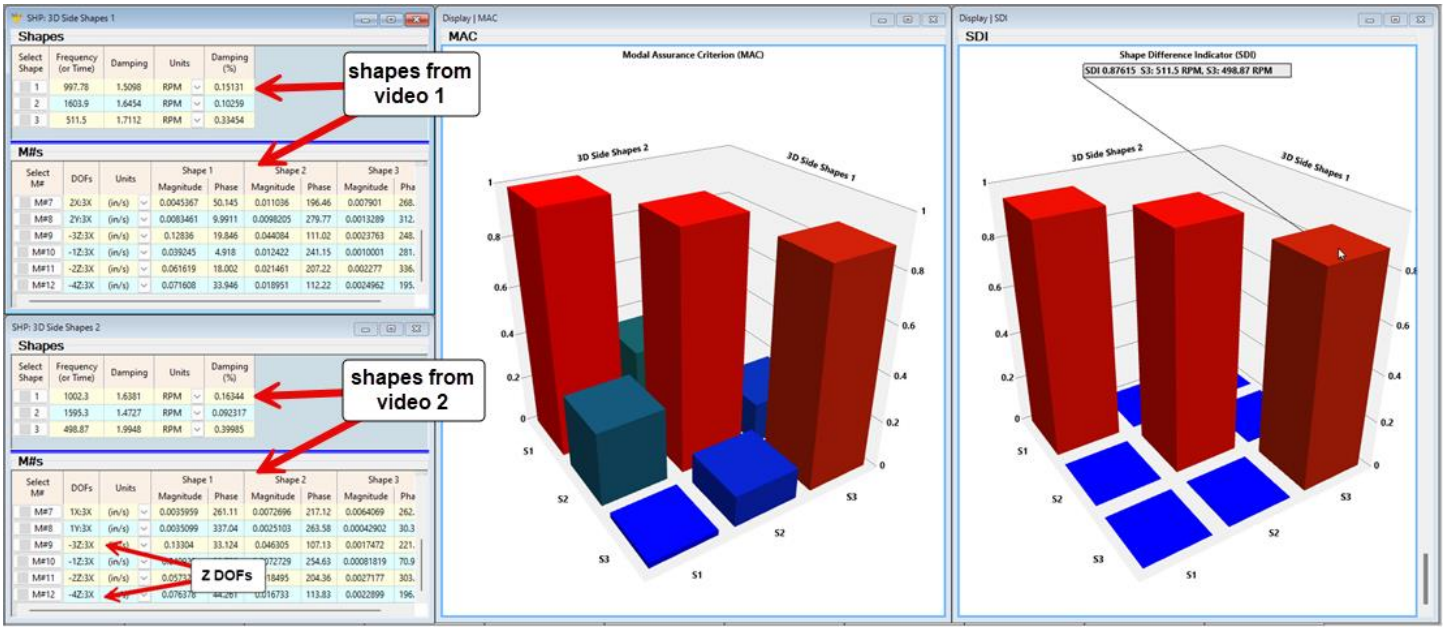

Figure 12. MAC & SDI - 3D Mode Shapes From Two Side View Videos

CONCLUSIONS

In this paper, we extracted **2D** mode shapes from two videos of the **Side** view and two from the **Top** view of a rotating machine while it was running at approximately **1000 RPM**. **TWFs** were extracted from the videos, and **ODS-FRFs** were calculated from the **TWFs** using ***5 spectrum averages*** and ***95% overlap processing***. Before the spectrum averaging, a **Hanning** window was applied to the **TWFs** to reduce signal leakage from the resonance peaks.

ODS-FRFs were calculated for two points on the motor and a point on the top of each bearing block. The **ODS-FRFs** contained three distinct resonance peaks, the first-order peak at ***about* 1000 RPM**, the aliased second-order peak at ***about* 1600 RPM**, and a machine resonance peak at ***about* 500 RPM**.

After the **ODS-FRFs** were windowed using a **Deconvolution** window, **2D** mode shapes of the rotating machine were identified by applying **FRF-based curve fitting** to the windowed **ODS-FRFs** from each video.

The mode shapes from the two videos for each view were then correlated using two correlation coefficients, the **Modal Assurance Criterion (MAC)** [7], and **Shape Difference Indicator (SDI)** [8]. All the mode shape pairs from the two videos correlated with coefficients ***about* 90%.**

3D mode shapes were then created by using components of the **2D** mode shapes because both the **Top** & **Side** view videos ***shared a common* X-axis** along the shaft of the machine. The common ***reference* DOF** (**3X**) was used in all the **ODS-FRF** calculations.

If all **ODS-FRFs** are calculated using ***the same reference* DOF**, then all magnitudes & phases are preserved among the **ODS-FRFs** and therefore among the mode shapes obtained by curve fitting the **ODS-FRFs**.

3D mode shapes of the **Side** view of the machine were created by adding the **Y**-direction components of the **2D** mode shapes from the **Top** view as **Z**-direction components of the mode shapes of the **Side** view. Likewise, **3D** mode shapes of the **Top** view were created by adding the **Y**-direction components of the **2D** mode shapes from the **Side** view as **Z**-direction components of the mode shapes of the **Top** view.

Finally, the **3D** mode shapes created for both the **Top** & **Side** views were correlated using the **MAC & SDI** correlation methods. All **3D** mode shapes correlated with values **above 90%, *but with one exception***. The **500 RPM** machine resonance mode shapes correlated with an **SDI** value of **88%,** meaning that the magnitudes & phases of that **3D** mode shape were ***slightly different*** from one another.

REFERENCES

[1] - S. Richardson, M. Richardson “Using Mode Shapes From Cell Phone Videos For Machinery Health Monitoring” VIATC 2025 Newport News, VA August 6-8, 2025

[2] - S. Richardson, M. Richardson “Extracting 3D Mode Shapes from a Cell Phone Video” IMAC XLII Orlando, FL February 10-13, 2025

[3] - D. Ambre, B. Schwarz, S. Richardson, M. Richardson, “Using Cell Phone Videos to Diagnose Machinery Faults” IMAC XLI Austin, TX February 13-16, 2023

[4] - B. Schwarz, S. Richardson, M. Richardson, “Using a Cell Phone Video and ODS Correlation to Diagnose Unbalance in Rotating Machinery” IMAC XLII Orlando, FL January 29-February 1, 2024

[5] - M.H. Richardson, “Is It a Mode Shape or an Operating Deflection Shape?” Sound and Vibration magazine March 1997

[6] - B. Schwarz, M.H. Richardson, “Measurements Required for Displaying Operating Deflection Shapes” Proceedings of IMAC XXII January 26, 2004

[7] - R.J. Allemang, D.L. Brown "A Correlation Coefficient for Modal Vector Analysis", IMAC Proceedings, pp.110-116, 1982

[8] - S. Richardson, J. Tyler, P. McHargue, M. Richardson “A New Measure of Shape Difference” IMAC XXXII February 3-6, 2014

[9] - S. Richardson, J. Tyler, B. Schwarz, P. McHargue, M. Richardson “Using Modal Parameters for Structural Health Monitoring” IMAC-XXXV Garden Grove, CA January 30-February 2, 2017

[10] - MEscope™ is a trademark of Vibrant Technology, Inc. www.vibetech.com